中国光学 Chinese Optics 核心期刊

高比探测率和高速石墨烯/n–GaAs复合结构的光电探测器

田慧军 刘巧莉 岳恒 胡安琪 郭霞

Hybrid graphene/n-GaAs photodiodes with high specific detectivity and high speed

TIAN Hui-jun, LIU Qiao-li, YUE Heng, HU An-qi, GUO Xia

引用本文:
田慧军, 刘巧莉, 岳恒, 胡安琪, 郭霞. 高比探测率和高速石墨烯/n–GaAs复合结构的光电探测器[J]. 中国光学, 2021, 14(1): 206–212. doi: 10.37188/CO.2020–0153
TIAN Hui-jun, LIU Qiao-li, YUE Heng, HU An-qi, GUO Xia. Hybrid graphene/n-GaAs photodiodes with high specific detectivity and high speed[J]. *Chinese Optics*, 2021, 14(1): 206-212. doi: 10.37188/CO.2020-0153

在线阅读 View online: https://doi.org/10.37188/CO.2020–0153

您可能感兴趣的其他文章

Articles you may be interested in

基于石墨烯的光学控制窄带太赫兹开关

Optically controlled narrowband terahertz switcher based on graphene

中国光学. 2018, 11(2): 166 https://doi.org/10.3788/CO.20181102.0166

石墨烯太赫兹波动态调制的研究进展

Recent progress in terahertz dynamic modulation based on graphene

中国光学. 2017, 10(1): 86 https://doi.org/10.3788/CO.20171001.0086

横向收集结构锗硅半导体雪崩探测器的设计研究

Design and research of Ge/Si avalanche photodiode with a specific lateral carrier collection structure

中国光学. 2019, 12(4): 833 https://doi.org/10.3788/CO.20191204.0833

集成PIN光敏元的CMOS探测器光电响应特性研究

Study on the photo response of a CMOS sensor integrated with PIN photodiodes

中国光学. 2019, 12(5): 1076 https://doi.org/10.3788/CO.20191205.1076

氧化石墨烯的多色发光及其在荧光成像中的应用

Multicolor fluorescent emission of graphene oxide and its application in fluorescence imaging

中国光学. 2018, 11(3): 377 https://doi.org/10.3788/CO.20181103.0377

基于Se和有机无机钙钛矿异质结的宽光谱光电探测器制备及其光电特性研究

Fabrication and photoelectric properties of organic–inorganic broad–spectrum photodetectors based on Se microwire/perovskite heterojunction

中国光学. 2019, 12(5): 1057 https://doi.org/10.3788/CO.20191205.1057

文章编号 2095-1531(2021)01-0206-07

Hybrid graphene/n-GaAs photodiodes with high specific detectivity and high speed

TIAN Hui-jun[1,2], LIU Qiao-li[2], YUE Heng[2], HU An-qi[2*], GUO Xia[2*]

(1. *Faculty of Materials and Manufacturing*, *Beijing University of Technology*, *Beijing* 100124, *China*;
2. *School of Electronic Engineering*, *Beijing University of Posts and Telecommunications*, *Beijing* 100876, *China*)

* *Corresponding author*, *E-mail*: *anqihu@bupt.edu.cn*; *guox@bupt.edu.cn*

Abstract: Hybrid graphene/semiconductor phototransistors have attracted great attention because of their ultrahigh responsivity. However, the specific detectivity (D^*) for such hybrid phototransistors obtained from source-drain electrodes is assumed to be 1/*f* noise. In this paper, D^* of ~1.82×10^{11} Jones was achieved from source-gate electrodes. Compared with the same device which was measured from source-drain electrodes, D^* was improved by ~500 times. This could be attributed to the carrier trapping and detrapping processes having been screened by the Schottky barrier at the interface. The rise and decay times were 4 ms and 37 ms, respectively. The temporal response speed also correspondingly improved by ~2 orders of magnitude. This work provides an alternative route toward light photodetectors with high specific detectivity and speed.

Key words: graphene; photodiode; specific detectivity; response speed

高比探测率和高速石墨烯/n-GaAs 复合结构的光电探测器

田慧军[1,2], 刘巧莉[2], 岳 恒[2], 胡安琪[2*], 郭 霞[2*]

(1. 北京工业大学 材料与制造学部, 北京 100124;
2. 北京邮电大学 电子工程学院, 北京 100876)

摘要: 混合结构的石墨烯/半导体光电晶体管因其超高的响应度而备受关注。然而, 该类光电晶体管通过源-漏电极测试得到的比探测率 (D^*) 容易受到 1/*f* 噪声的限制。本文制备了混合结构的石墨烯/GaAs 光电探测器, 通过源-栅电极测得 D^*大约为 1.82×10^{11} Jones, 与通过源-漏电极测量相比, D^*提高了约 500 倍。这可归因于界面上肖特基势垒对载流子俘获和释放过程的屏蔽作用。此外, 探测器的上升时间和下降时间分别是 4 ms 和 37 ms, 响应速度相应地提高了 2 个数量级。该工作为制备高比探测率和高速的光电探测器提供了一种新的思路。

关 键 词: 石墨烯; 光二极管; 比探测率; 响应速度

中图分类号: TN364 **文献标志码:** A **doi:** 10.37188/CO.2020-0153

收稿日期: 2020-09-01; **修订日期:** 2020-09-14

基金项目: 国家重点研发计划资助项目(No. 2017YFF0104801); 国家自然科学基金资助项目(No. 61804012)

Supported by the National Key Research and Development Program of China (No. 2017YFF0104801); National Natural Science Foundation of China (No. 61804012)

1 Introduction

Graphene with atomic layer thickness has attracted worldwide attention because of its unique electronic, optoelectronic, mechanical properties[1,2]. Recently, hybrid graphene/semiconductor phototransistors have been increasingly investigated for optoelectronic applications because of their ultrahigh responsivity[3-5]. In such structures, photogenerated carriers separate at the interface of the graphene/semiconductor junction. Because of the photogating effect, the responsivity obtained via such photoconductivity-based devices, whose photocurrent was measured from source-drain electrodes, can be as high as 10^{10} A/W at 0.19 V[6]. The corresponding specific detectivity (D^*), which characterizes the sensitivity of a photodetector, has been reported to be as high as 1.4×10^{12} Jones[6]. However, based on a detailed comparison of the magnitude of three types of noise[6,7], it can be found that the D^* of such phototransistors is mainly limited by $1/f$ noise[6], not the thermal noise or the shot noise, which play dominant roles in conventional photovoltaic-type semiconductor photodiodes[7-8]. The $1/f$ noise in this system mainly originates from the carrier trapping and detrapping processes at the graphene/semiconductor interface[9]. In other words, the D^* of photoconductivity-based devices ranges from ~10^8 Jones to ~10^{14} Jones, which brings great enhancement in responsivity[3-6]. A high density of trapping centers at the interface also results in severe persistent photoconduction, and a relatively long transient response time. Generally, the reported transient response time of such hybrid phototransistors is in the order of seconds or even milliseconds[5,6]. These photodetectors need to work under external bias voltage, whose applications are usually limited because of the large $1/f$ noise. To overcome these limitations, new types of photodetectors are required[10].

For the direction perpendicular to the graphene/semiconductor junction, whose photocurrent is measured by source-gate electrodes, interface traps play only a small role in the entire current transport loop. The source of $1/f$ noise is lessened and the persistent photoconductive effect can be relieved, which induces a high D^* and high response speed[11]. These photodetectors with low power consumption, low cost and high sensitivity can satisfy practical applications ' requirements such as in visible light imaging and large-scale integrated circuitry[12,13]. For photovoltaic-type devices, the D^* ranges from ~10^{10} Jones to ~10^{13} Jones, which originates from there being lower noise under zero voltage[10]. Moreover, the reported transient response time of photovoltaic-type devices is in the order of microseconds[11]. In this paper, the photocurrent measured from the source-gate electrodes of a hybrid graphene/n-GaAs photodiode demonstrated improved D^* and response speed. This work is promising for developing low power consumption visible-light photodetectors with high sensitivity that are ideal in applications like imaging.

2 Materials and methods

Si doped with a GaAs substrate with an electron concentration of ~1×10^{18} cm^{-3} was selected for this study. Au/Ge/Ni/Au (10/10/5/100 nm) electrodes were deposited on the back of the n-GaAs substrate and then treated via rapid thermal annealing at 430 ºC for 35 s in an N_2 environment to form ohmic contact[14]. The graphene was synthesized via chemical vapor deposition on Cu foil and then transferred to the front of the GaAs substrate using polymethylmethacrylate (PMMA) as the supporting film. Thus, a hybrid graphene/n-GaAs photodiode was obtained after metal deposition. The Raman spectrum was tested using a Renishaw Invia Raman microscope with a 514-nm laser source. Electrical measurements were carried out using a Keithley 4 200. Illumination was provided by a laser at 650 nm with a series of neutral density filters under ambient

conditions. A Si photodiode (Hamamatsu S2387) was used to calibrate the power.

3 Results and discussion

Figure 1(a) demonstrates the schematic diagram of the graphene/n-GaAs photodiode studied in this work. The optical and electrical performances were measured from source-gate electrodes at room temperature. Figure 1(b) illustrates the energy band diagram of the graphene/n-GaAs heterojunction, where a Schottky barrier forms at the interface. Because of the different work functions between graphene (~4.8 eV) and n-GaAs (~4.1 eV)[15-16], the energy band bends upward and a built-in electric field is formed at the interface between graphene and n-GaAs with a barrier height of ~0.7 eV. The photoexcited electron-hole pairs separate under the function of the built-in field when light illuminates the sample. Due to the high surface state density of the GaAs material, the photoexcited holes fill up its surface states first because they accumulate near the interface, as illustrated in Figure 1(b). The Raman spectrum of the graphene is as shown in Figure 1(c). The G and 2D bands are located at 1 582.9 cm^{-1} and 2 683.8 cm^{-1}, respectively. The absence of a D band indicates that there are few defects[17]. The intensity ratio of the 2D band to the G band is above 3, which causes monolayer characteristics of graphene[18]. Figure 1(d) shows the spectral response of the device. Under a zero bias voltage, the spectral responsivity of the photodiode was shown for an incident light power of ~200 nW over the range of 300~1 100 nm. The responsivity exceeded 75 mA/W in the visible light region (380~760 nm). The cutoff wavelength was around 870-nm which corresponded to the GaAs edge of the energy band.

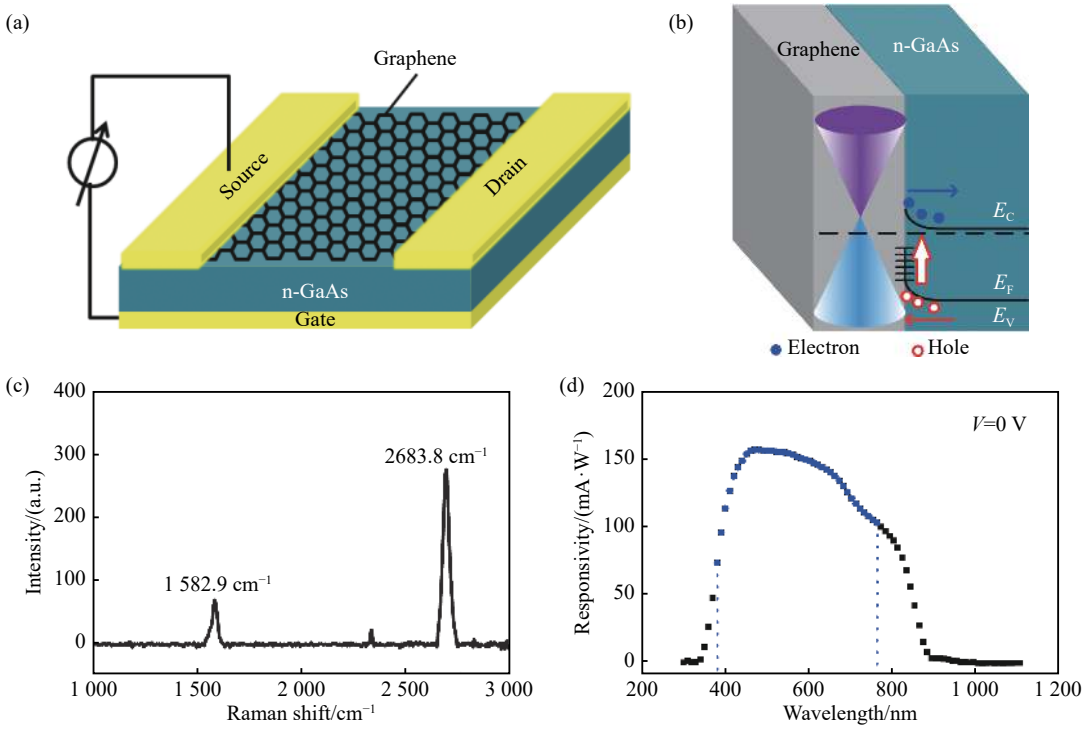

Fig. 1 (a) Schematic diagram of the graphene/n-GaAs photodetector. The optical and electrical performances were measured by source-gate electrodes. (b) Energy band diagram of the graphene/n-GaAs heterojunction with the Schottky barrier height Φ_B of the graphene/GaAs junction of ~0.7 eV. The interface states are depicted at the interface, illustrating that the carrier trapped photons at the graphene/GaAs interface during carrier transport through the junction. (c) Measurement result of the Raman spectrum of graphene on the GaAs substrate. (d) Spectral response of the photodiode under zero bias voltage.

Figure 2(a) (Color online) shows the current-voltage (*I-V*) measurement results of the photodiodes illuminated under a 650-nm laser with different light intensities. All the curves demonstrate good rectification behavior due to the heterojunction formed between graphene and n-GaAs[19]. According to thermionic emission theory, current-voltage curves are expressed as below:

$$I = I_0\left[\exp\left(\frac{qV}{nkT}\right)-1\right] \quad , \qquad (1)$$

$$I_0 = AA^*T^2\exp\left(\frac{-q\Phi_B}{kT}\right) \quad , \qquad (2)$$

where q is the charge, V is the bias voltage, k is the Boltzmann constant, T is the temperature, n is the ideality factor, I_0 is the reverse saturation current, A is the photosensitive area of the photodiode, A^* is the effective Richardson constant of n-GaAs (12.1 $A\cdot K^{-2}cm^{-2}$)[18], and Φ_B is the barrier height of the Schottky junction[20-21]. According to the fitting results, Φ_B and n were respectively extracted to be 0.65 eV and 1.89 for the dark curve, which is almost consistent with the above theoretically determined value. The extracted data of n, which is much larger than 1, indicates that the recombination process with the assistance of interfacial states dominates the carrier transport process at the graphene/GaAs interface.

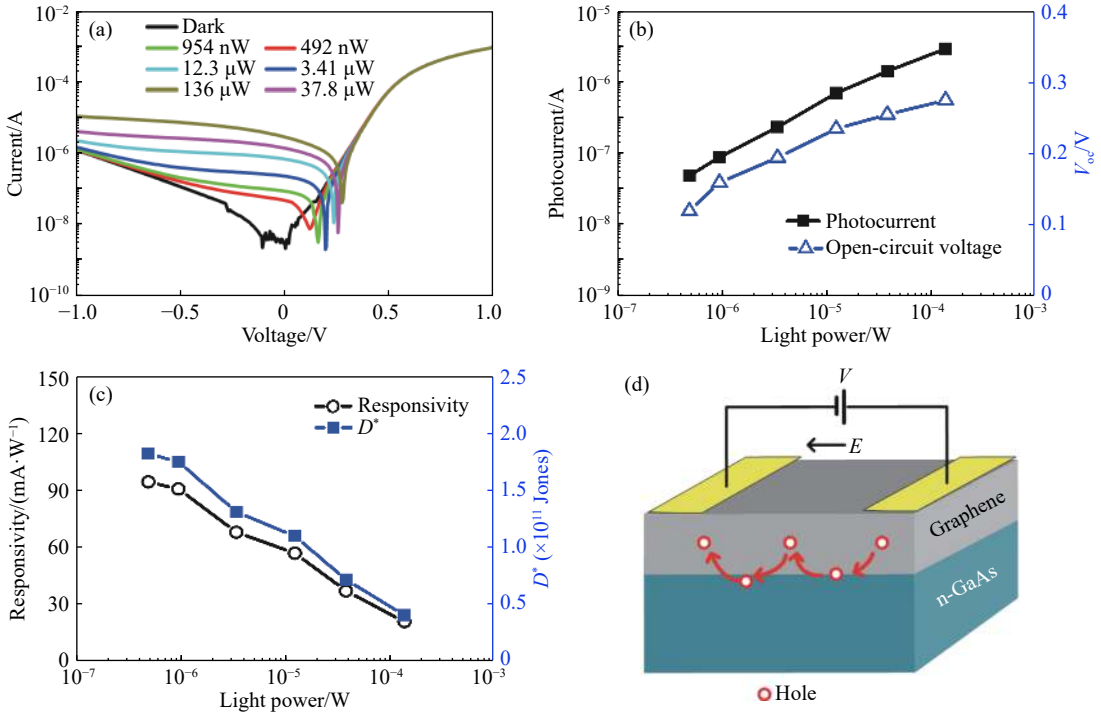

Fig. 2　(a) Current versus voltage curves of the device under different light powers. (b) The relationship between photocurrent and photovoltage (V_{oc}) with the incident light's power in the self-driven mode. (c) Responsivity and D^* versus illumination power under a zero bias voltage. (d) Illustration of the carrier trapping and detrapping processes at the interface of the graphene/GaAs interface, which is the main source of 1/*f* noise.

The photocurrent (I_{photo}) increases linearly from 49.7 nA to 2.93 μA as the illumination power increased from 492 nW to 136 μW at a zero bias voltage, as shown in Figure 2(b). The photovoltage (V_{oc}) increased from 0.12 to 0.275 V when the power increased from 492 nW to 136 μW. Figure 2(c) shows the responsivity versus the power of the incident light of the device. The responsivity (R) of the photodiode is defined by the equation

$$R = I_{photo}/P_{in} \quad , \qquad (3)$$

where P_{in} is the incident light power. Under a zero bias voltage, the highest responsivity was 95 mA/W. It can be seen that the responsivity of the photodi-

ode slightly decreased with an increase in power. This can be attributed to a reduction in the built-in field when there is an increasing number of photo-generated carriers, which forms an electric field that opposes the built-in field. When light illuminates the graphene/n-GaAs photodetector, GaAs absorbs the photons with energy larger than its bandgap and induces electron-hole pairs, which are separated by the function of the built-in field. Photo-induced holes move towards graphene, while photo-induced electrons move towards GaAs. The photo-induced holes fill up the surface states first because of the high surface state density of the GaAs material. Then the other photo-induced holes can be driven into graphene and collected by the electrode to generate the photoresponse.

D^* is one of the important parameters for a photodetector, which is defined as

$$D^* = (AB)^{1/2}/P_N \quad , \qquad (4)$$

where A is the area (0.01 cm^2) of the device, B is the electrical bandwidth, and P_N is the noise's equivalent power. P_N is expressed as

$$P_N = (S_I)^{1/2}/R \quad , \qquad (5)$$

where R is the responsivity and S_I is the mean-square of the noise's current in the dark. According to the theory of noise, S_I is the total sum of the 1/f noise (S_I(1/f)), the shot noise (S_I(shot)), and the thermal noise (S_I(thermal))[22], which can be calculated using

$$S_I = S_I(1/f) + S_I(\text{shot}) + S_I(\text{thermal}). \qquad (6)$$

At a modulation frequency of 1 Hz, the $S_I(1/f)$ is ~10^{-35} A^2·Hz^{-1}, which can be represented by the following equation:

$$S_I(1/f) = \frac{|I(f)|^2}{F_S N} \quad , \qquad (7)$$

where $I(f)$ is the discrete Fourier transform of the dark current waveform $I(t)$, F_S is the sampling rate, and N is the number of data points. The S_I(shot) is calculated to be ~1.04×10^{-27} A^2·Hz^{-1} by using

$$S_I(\text{shot}) = 2qI_d \quad , \qquad (8)$$

where q is the elemental charge and I_d is the dark current of the device. S_I (thermal) is calculated to be ~1.66×10^{-27} A^2·Hz^{-1} at room temperature by using Nyquist's equation, represented as

$$S_I(\text{thermal}) = 4kT/R_S \quad , \qquad (9)$$

where k is the Boltzmann constant, T is the temperature, and R_S is the differential resistance of the device in the dark. As shown in Figure 2(c), D^* at 0 V was observed to decrease with increasing light power because of the reduction of responsivity. The maximum D^* of the device was 1.82×10^{11} Jones, which is 562 times higher than the source-drain signal of a graphene/GaAs phototransistor that was fabricated in the same experiment conditions[11]. The obvious improvement of D^* is attributed to the screen effect from the Schottky barrier. Comparing the two types of carrier transport processes, as illustrated in Figure 2(d) and 1(b), the 1/f noise dominates the mean square noise S_I for the source-drain photocurrent because of the trapping and detrapping processes at the interface during carrier transport, which is related to the carrier number and mobility fluctuation[9]. The 1/f noise of the source-gate measurement, as illustrated in Figure 1(b), was cut off because the interfacial states were filled by photoexcited holes first. Only then were the other photoexcited holes allowed the transport electrodes. The trapping barrier can be lowered only at elevated temperatures and bias. Because the source of noise was changed from well-known 1/f noise to thermal noise, D^* improved greatly.

Figure 3 shows the transient response measurement of the device under a laser power of 136 μW at 0 V at room temperature[23]. It should be noted that there is a peak when the light turns on, which can be repeated. We attributed it to the pyroelectricity effect caused by the electrical response to a sudden tiny temperature change when the light was turned on[24]. The rise time (τ_r) and decay time (τ_f) were measured to be 4 ms and 37 ms, respectively. The relatively long decay time after switching off the light indicates that it took more time for carriers to

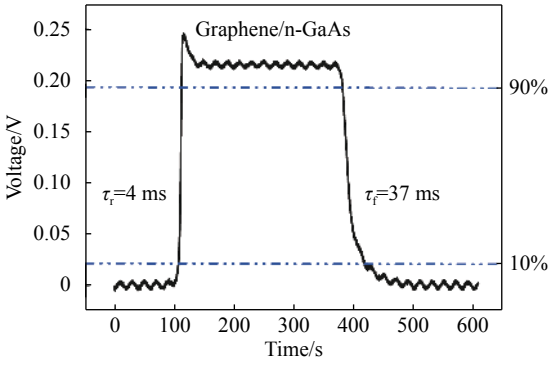

Fig. 3　The response time of the photodiode at a zero bias voltage under a laser power of 136 μW where τ_r is ~4 ms and τ_f is ~37 ms.

be transported from the GaAs semiconductor to the depletion region via diffusion and then be injected into graphene and recombined. The fast response was attributed to the quick separation of photogenerated carriers by the built-in electric field at the interface. Compared with the results measured by source-drain electrodes, which respectively had a rise and decay time of 270 ms and 28.5 s[11], the transit response performance also improved by ~2 orders of magnitude.

4　Conclusion

In this work, the optoelectronic performance of the graphene/n-GaAs structure measured by source-gate electrodes was described. Due to the trapping and detrapping processes, there was a maximum specific detectivity of 1.82×10^{11} Jones with a rise time of 4 ms and a decay time of 37 ms, achieved at 0 V at room temperature. We attribute the ~2 orders of magnitude improvement in specific detectivity and its corresponding response time to the screening of interfacial states given by the Schottky barrier.

参考文献：

[1] KOPPENS F H L, MUELLER T, AVOURIS P, *et al*.. Photodetectors based on graphene, other two-dimensional materials and hybrid systems[J]. *Nature Nanotechnology*, 2014, 9(10): 780-793.

[2] NAIR R R, BLAKE P, GRIGORENKO A N, *et al*.. Fine structure constant defines visual transparency of graphene[J]. *Science*, 2008, 320(5881): 1308.

[3] GUO X T, WANG W H, NAN H Y, *et al*.. High-performance graphene photodetector using interfacial gating[J]. *Optica*, 2016, 3(10): 1066-1070.

[4] GREBENCHUKOV A N, ZAITSEV A D, KHODZITSKY M K. Optically controlled narrowband terahertz switcher based on graphene[J]. *Chinese Optics*, 2018, 11(2): 166-173.

[5] HU A Q, TIAN H J, LIU Q L, *et al*.. Graphene on self-assembled InGaN quantum dots enabling ultrahighly sensitive photodetectors[J]. *Advanced Optical Materials*, 2019, 7(8): 1801792.

[6] LIU Q L, TIAN H J, LI J W, *et al*.. Hybrid graphene/Cu_2O quantum dot photodetectors with ultrahigh responsivity[J]. *Advanced Optical Materials*, 2019, 7(20): 1900455.

[7] GONG X, TONG M H, XIA Y J, *et al*.. High-detectivity polymer photodetectors with spectral response from 300 nm to 1450 nm[J]. *Science*, 2009, 325(5948): 1665-1667.

[8] WANG G SH, LU H, CHEN D J, *et al*.. High quantum efficiency GaN-based p-i-n ultraviolet photodetectors prepared on patterned sapphire substrates[J]. *IEEE Photonics Technology Letters*, 2013, 25(7): 652-654.

[9] BALANDIN A A. Low-frequency 1/*f* noise in graphene devices[J]. *Nature Nanotechnology*, 2013, 8(8): 549-555.

[10] LU Y H, FENG S R, WU ZH Q, *et al*.. Broadband surface plasmon resonance enhanced self-powered graphene/GaAs photodetector with ultrahigh detectivity[J]. *Nano Energy*, 2018, 47: 140-149.

[11] TIAN H J, HU A Q, LIU Q L, *et al*.. Interface-induced high responsivity in hybrid graphene/GaAs photodetector[J]. *Advanced Optical Materials*, 2020, 8(8): 1901741.

[12] 胡伟达, 李庆, 陈效双, 等. 具有变革性特征的红外光电探测器[J]. 物理学报, 2019, 68(12): 120701.
HU W D, LI Q, CHEN X SH, *et al*.. Recent progress on advanced infrared photodetectors[J]. *Acta Physica Sinica*, 2019, 68(12): 120701. (in Chinese)

[13] CHEN Y Y, WANG C H, CHEN G S, *et al*.. Self-powered n-$Mg_xZn_{1-x}O$/p-Si photodetector improved by alloying-enhanced piezopotential through piezo-phototronic effect[J]. *Nano Energy*, 2015, 11: 533-539.

[14] FAUSKE V T, HUH J, DIVITINI G, *et al*.. In situ heat-induced replacement of GaAs nanowires by Au[J]. *Nano Letters*, 2016, 16(5): 3051-3057.

[15] ZHANG X T, ZHANG L N, CHAN M S. Doping enhanced barrier lowering in graphene-silicon junctions[J]. *Applied Physics Letters*, 2016, 108(26): 263502.

[16] LI X Q, LIN SH SH, LIN X, *et al*.. Graphene/h-BN/GaAs sandwich diode as solar cell and photodetector[J]. *Optics Express*, 2016, 24(1): 134-145.

[17] CANCADO L G, JORIO A, FERREIRA E H M, *et al*.. Quantifying defects in graphene via Raman spectroscopy at different excitation energies[J]. *Nano Letters*, 2011, 11(8): 3190-3196.

[18] HAO Y F, WANG Y Y, WANG L, *et al*.. Probing layer number and stacking order of few-layer graphene by Raman spectroscopy[J]. *Small*, 2010, 6(2): 195-200.

[19] DI BARTOLOMEO A. Graphene Schottky diodes: an experimental review of the rectifying graphene/semiconductor heterojunction[J]. *Physics Reports*, 2016, 606: 1-58.

[20] TONGAY S, LEMAITRE M, MIAO X, *et al*.. Rectification at graphene-semiconductor interfaces: zero-gap semiconductor-based diodes[J]. *Physics Review X*, 2012, 2(1): 011002.

[21] LIN F, CHEN SH W, MENG J, *et al*.. Graphene/GaN diodes for ultraviolet and visible photodetectors[J]. *Applied Physics Letters*, 2014, 105(7): 073103.

[22] NI ZH Y, MA L L, DU S CH, *et al*.. Plasmonic silicon quantum dots enabled high-sensitivity ultrabroadband photodetection of graphene-based hybrid phototransistors[J]. *ACS Nano*, 2017, 11(10): 9854-9862.

[23] ZENG L H, WU D, LIN SH H, *et al*.. Controlled synthesis of 2D palladium diselenide for sensitive photodetector applications[J]. *Advanced Functional Materials*, 2019, 29(1): 1806878.

[24] MEIRZADEH E, CHRISTENSEN D V, MAKAGON E, *et al*.. Surface pyroelectricity in cubic SrTiO3[J]. *Advanced Materials*, 2019, 31(44): 1904733.

Author Biographics:

TIAN Hui-jun (1984—), PhD student, Institute of Laser Engineering, Beijing University of Technology, China. His research interests focus on graphene-based photodetectors. E-mail: tianhj@emails.bjut.edu.cn

GUO Xia (1974—), Professor, School of Electronic Engineering, Beijing University of Posts and Telecommunications, China. Her research interests are on high-response PIN diodes, high speed VCSELs and ultrahigh-sensitive photodetectors in Graphene. E-mail: guox@bupt.edu.cn